Electronic Supplementary Information

Layer-by-layer Assembled Membranes with Immobilized Porins

Sebastián Hernández[1], Cassandra Porter[1], Xinyi Zhang[2], Yinan Wei[2] and Dibakar Bhattacharyya[1]

[1]Department of Chemical and Materials Engineering, University of Kentucky, Lexington, KY

[2]Department of Chemistry, University of Kentucky, Lexington, KY

*Corresponding author
Prof. D. Bhattacharyya
University Alumni Chair Professor
Dept. of Chemical and Materials Engineering
University of Kentucky
177 F. Paul Anderson Tower
Lexington, KY 40506-0046
Email: db@uky.edu

1. Other OmpF Solution Characterizations

OmpF work as permeable barriers that transport small molecules through the cell membrane.[1] It has weak cation activity and can selectively filter hydrophilic molecules smaller than 600 Da.[2] Native OmpF is a trimer with each monomer forming a 16-stranded anti-parallel β-barrels.[3] The hydrophobic interaction between monomers stabilize the trimer conformation of OmpF, which is stable even in organic solvents, except phenol.[4] There are several methods to determine protein concentration. Aromatic amino acids like tyrosine and tryptophan absorb UV light at 280 nm. Therefore, protein concentration can be calculated through Beer's law. This method is easy and quick; however, it is only accurate when aromatic amino acids are exposed. The Bradford assay, for example, is a colorimetric assay based on the interactions between Coomassie brilliant blue G-250 and the arginine and aromatic residues. The maximum absorption of Coomassie brilliant blue G-250 shifts from 470 nm to 595 nm when binding with these residues. Similarly, to measure absorbance at 280nm, Bradford assay requires a decent number of aromatic and arginine residues. Besides, basic conditions or detergents such as SDS can inhibit the dye that binds to the protein. On the other hand, the enhanced BCA assay is also a colorimetric assay based on the redox reaction between protein backbone and Cu^{2+}. When protein backbone reduces Cu^{2+} to Cu^+, bicinchoninic acid (BCA) binds with Cu^+ to form a complex that absorbs at 562 nm. Reducing reagents are not involved during the OmpF purification steps described. In addition, the enhanced BCA assay is not sensitive to detergents and denaturants, interacts with peptide backbone, and is less sensitive to the amino acids present.

2. Membrane Functionalization and Characterization

PVDF membranes with a top surface area of 13.2 cm^2 were soaked 10 min in deionized ultra-filtered water (DIUF) and dried in an oven set to 50 °C for 5 min. A monomer solution of acrylic

acid (AA) 1:10 by weight (1.26 M AA) was prepared with 1 mol% relative to AA each of potassium persulfate (KPS) as initiator and N,N'-Methylenebisacrylamide (MBA) as cross-linker. To prevent premature polymerization, KPS was separately dissolved in half of the DIUF used, then combined with the monomer solution right before soaking membranes for 10 minutes. Vacuum was used to pull partially the monomer solution through the membrane to ensure pores were completely filled.

Afterwards, the membranes were sandwiched and clipped between two plastic sheets and Teflon plates, put in a preheated oven with venting nitrogen for about 1.25 hours at 80°C and another 30 min without the Teflon plates for complete polymerization. The PVDF-PAA membranes were washed to remove unreacted species and dried at 50 °C for 10 min. The number of carboxylic groups (COOH) present on the membrane are calculated from the mass gain after functionalization using the molecular weight of repeating units of the monomer. This mass gain was used to calculate the amount of material needed to flux through in the subsequent PAH layer.

The pH of the PAH solution was adjusted to ~9.0 using NaOH to deprotonate the PAA in order to bond the amine groups of PAH to the COO^- groups. The prepared PAH solution was permeated twice for full polymer pickup. For the final top layer of PSS, 25 mL of DIUF containing a number of PSS repeat units equal to the COOH groups was prepared. The PSS had a chain length of 721 repeat units long. The solution was permeated through the membrane twice, at 10.2 bar and pH=6.0. A slightly acidic pH causes extracellular OmpF loops to be positively charged in general, which will have affinity with the carboxylic groups in PSS.

3. Surface Zeta (ζ) Potential

Surface ζ potential of a PV200 membrane with each additional functionalization layer was measured with a ζ potential analyzer (Anton-Paar Surpass Electrokinetic Analyzer). Samples were cut and mounted to two sample platforms with double-sided tape on the membrane backing. All runs started at a pH ≈ 5.2 with a solution of 0.05 M KCl and target pressure of 300 mbar; the gap between mounting platforms was adjusted to reach this pressure. First, an acidic measurement for a given sample was taken using HCl to adjust the pH gradually lower than 5.2. The process was repeated for basic measurements using NaOH for gradual adjustment above the starting pH. Acidic pH was tested separately from basic to avoid reaching large ionic strength of passing solution. Acidic and basic measurements were combined for each membrane type.

4. Characterization of Feed, Retentate and Permeate Solutions

A Total Organic Carbon Analyzer (TOC-5000A by Shimadzu) was used to create calibration curves for the measurement of concentrations of carbon-based molecules; because TOC measurement relies heavily on the performance of the syringe pump, the curves were checked before each day of use against a known concentration of potassium hydrogen phthalate. TOC as a method of determining rejection was verified by checking concentrations of glucose against those measured with a simple glucose meter (ReliOn Prime) used by diabetics to monitor blood sugar level. This meter uses glucose dehydrogenase meter strips instead of glucose oxidase-based strips, avoiding the error associated with oxidase's sensitivity to dissolved oxygen.[5] A second verification method was to check concentrations of Dextran Blue 5000 using UV-vis Spectrophotometer (UV-6300PC Double Beam Spectrometer by VWR). With calculated rejections between TOC methods and glucose-meter and UV-vis measurements falling within the

standard error of the mean of each other, TOC was deemed an accurate method for all other carbon-based molecules.

5. Membrane Selection

The microfiltration poly(vinylidene fluoride) (PVDF) membranes by Nanostone that were first considered in this study possessed different fluxes and pore size distributions. First, as shown in Table S1, a sponge-like membrane with a different concentration of AA was considered (XPVDF) but due to its thickness and low flux, it was discarded expecting higher pore clogging once the other layers were placed onto it.

Table S1. Flux, mass gain and carboxylic functionalization values of different PVDF (Nanostone) membranes with AA : H2O ratio of 1:15 w/w.

Membrane	Pure water Flux without PAA (LMH) at 2.04 bar	Mass without PAA (g)	Mass with PAA (g)	# of Carboxylic Groups (mmol)
XPVDF	93.6	0.2654	0.2851	0.27
PV200	700.2	0.1817	0.2102	0.39
PV700	2182.3	0.1572	0.2007	0.60

Here we compare both PV200 and PV700. Since PV200 was selected for the main study, refer to the subsection 3.2 in the main article for its characterization. The next considered membrane was the PV700 due to its higher flux and functionalization values. Samples of PVDF and polycarbonate (PC) membranes were cut to size for a Scanning Electron Microscope (SEM), mounted, coated with gold, and imaged. Care was taken to procure the optimal voltage and current combination for a focused image of the pores. Figure S1a shows the SEM image of PV700. Using ImageJ to measure pore perimeter and idealize pores into perfect cylinders to calculate an effective diameter, the average pore diameter of PV700 was 35 ± 20 nm. The large standard deviation indicates PV700 and PV200 (Figure 4 in main document) possess pores of

large variation. Figure S1b derived from the samples in the SEM images, depicts the histogram of PV700 pore sizes. PV700 has a distribution skewed toward lower values, with a significantly dominant population residing in 18.6-26.0 nm bin. PV200 in Figure 4 of the article also has fewer, more evenly distributed pores than PV700 and has a more normal distribution than the other membranes imaged, with higher populations toward the mean value, indicating more consistent pore sizes.
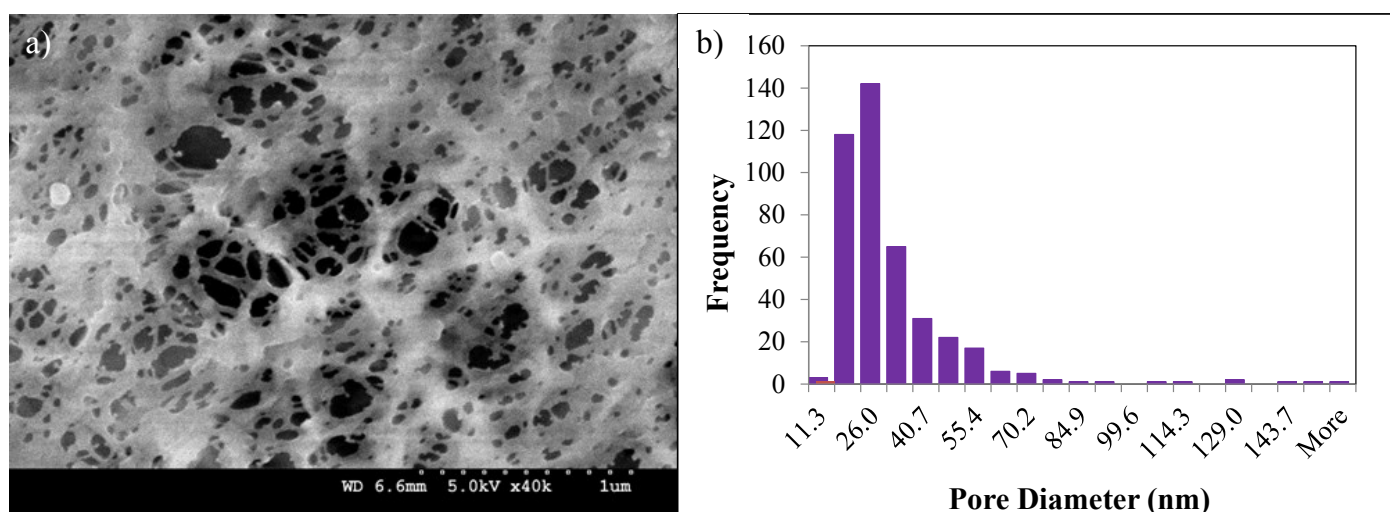
Figure S1. PVDF membrane characterization. (a) Top surface PVDF (Nanostone PV700), (b) Pore size distribution of PVDF (Nanostone PV700).

Still, perhaps the most influential pores in each membrane are the largest, as these dictate what particles are rejected or selected by the membrane; analogously, a nanofiltration membrane with the tightest pores available will reject nothing if it has a tear. Although PV700's highly populated bins are lower values than the most populated size bins of PV200 (see Figure 4 in the main article), its biggest pores are actually significantly larger. In the two samples taken, PV200's largest pore measured had a diameter of 149 nm while PV700's largest pore was 181 nm. The top largest 1% of measured pores from PV200 had an average diameter of 126 ± 16 nm while PV700's biggest 1% averaged 158 ± 17 nm. PV700's largest 1% exceeded that of PV200's

by a whopping 25% while its average pore diameter was 27% lower. Such a large gap between pore size median and maximum made PV700's membrane initially less attractive for immobilizing biomolecules that come in definitive individual and aggregate sizes. During PAA functionalization, the benefits of PV200 stood out and are discussed in the main article.

6. Optimization of Functionalization with PAA

Poly(acrylic acid) was initially functionalized onto the chosen PVDF membranes (PV200) at proportion of 1 gram AA to 5 grams water (2.31 M of AA) with KPS and (MBA) as initiator and cross-linker, respectively. However, this quantity of AA was shown to diminish water permeation at a pH ≈ 7 and 4.08 bar from 968 ± 63 LMH/bar in the non-functionalized PVDF membrane to only 7.7 ± 1.8 LMH/bar. Such low flux required that at least ten hours for the subsequent second functionalization layer via convective flow of dissolved PAH. Pores were extremely tight with PAA-PAH functionalization, resulting in water permeation (pH ≈ 7 and 4.08 bar) of 0.45 LMH/bar. Such tight pores likely could not hold OmpF aggregates; at the proportions of water, acid, and NaOH used in the OmpF solution.

Trials with mass proportions of AA to water of 1:7.5, 1:10 and 1:20 revealed that 1:7.5 still produced a tight membrane, 1:10 allowed for observable functionalization of PVDF, verified by using pH studies and mass-gain, and 1:20 showed no observable functionalization in PVDF, see Figure S2. Functionalization is desirable to provide charges to help stabilize the immobilization of OmpF. Our research group has previously shown that LbL assembly can increase immobilization of biomolecules by 25-fold.[6] Average water flux through 1:10 (1.26 M AA) promised a high likelihood that subsequent functionalization with PAH would result in pore sizes that were fitting for immobilization of OmpF aggregates.
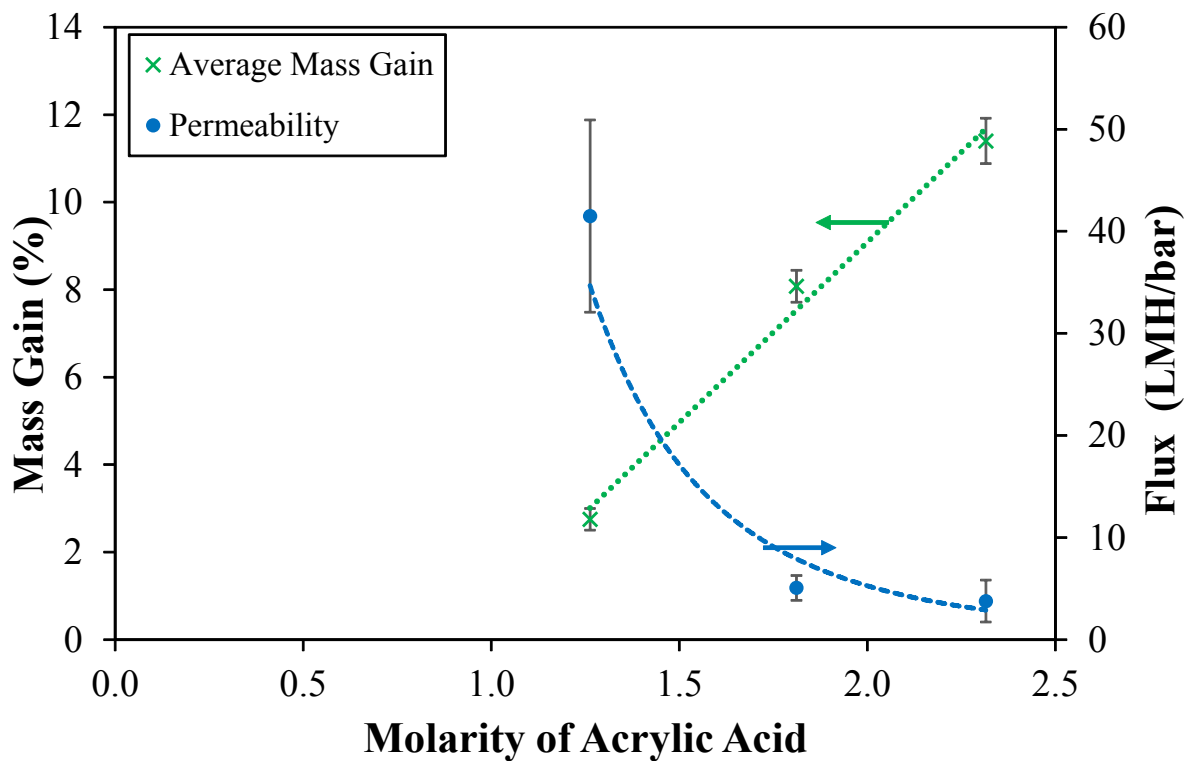
Figure S2. Concentrations of acrylic acid before polymerization as a function of mass gain of polymer in membrane and respective flux.

7. Model Organic Compound Regressions of Molecular Weights and Sizes
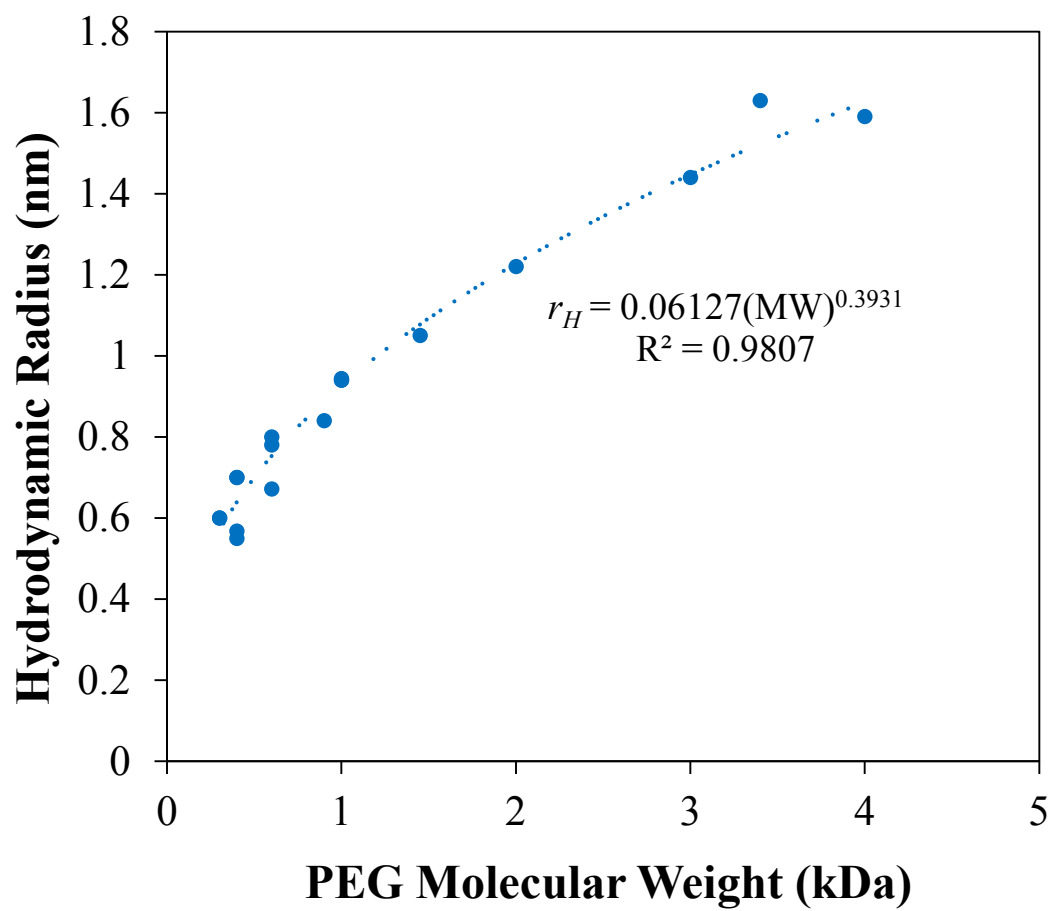
Figure S3. Regression of molecular weights vs. hydrodynamic radius of PEG.[7-9]

The plot shows:

$$r_H = 0.06127(MW)^{0.3931}$$
$$R^2 = 0.9807$$

Axis labels: Hydrodynamic Radius (nm) vs. PEG Molecular Weight (kDa)
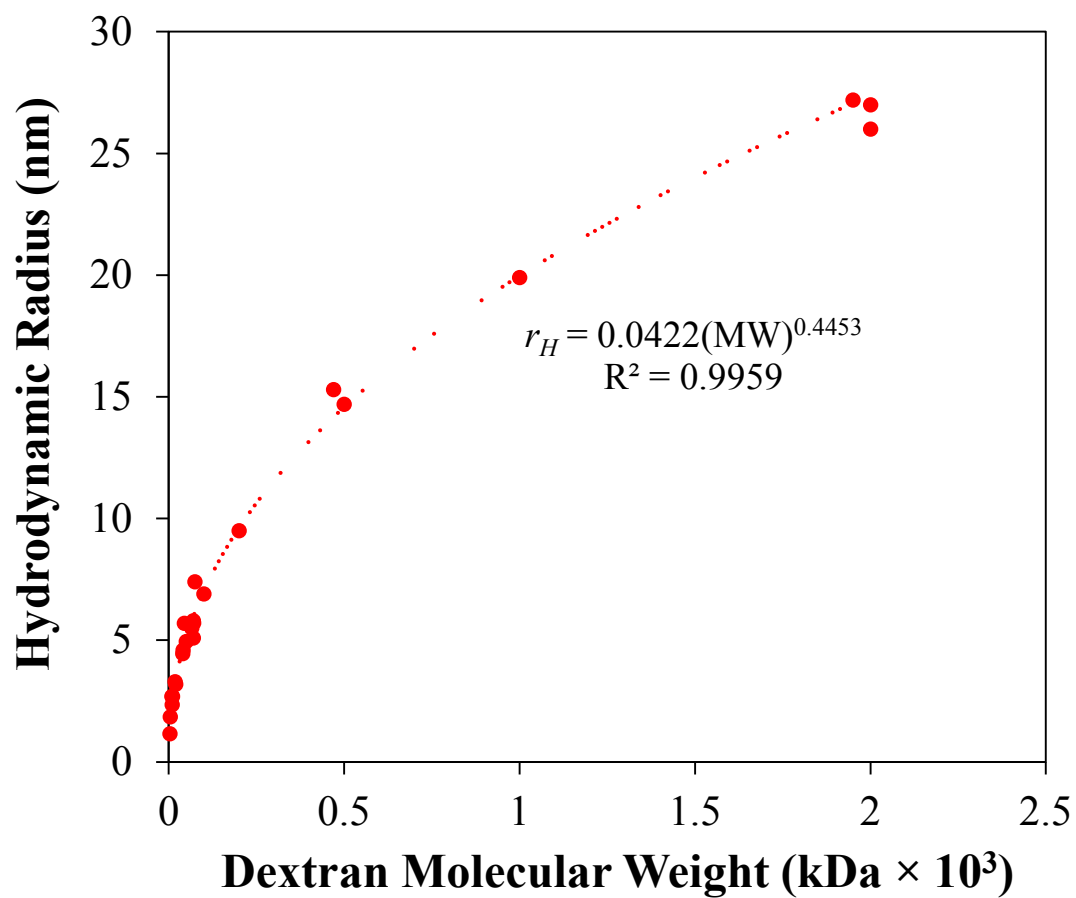
Figure S4. Regression of molecular weights vs. hydrodynamic radius of Dextran.[10-13]

8. Fluorescence Measurements
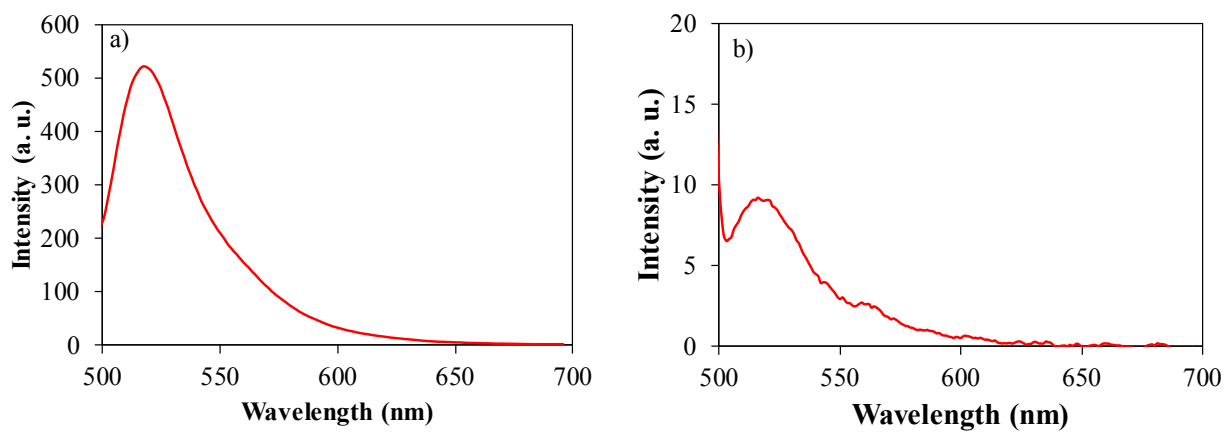
Figure S5. Spectra of FITC Labelled OmpF solutions. (a) Feed solution; (b) permeate solution.

Note the y-axis (intensity) Scale difference between (a) and (b). FITC emission is around 520

nm.

9. Material Imbalance Minimization

Although the deviation from the mass conservation due to measurements and/or absorption of the species within the membranes are somewhat low (absolute 8%), it is important to minimize these results in order to calculate batch operation processes. The mass conservation equations including imbalances are:

$$V_0 - V_P - V = I_V \tag{S1}$$

$$V_0 C_0 - V_P C_P - VC = I_C \tag{S2}$$

where V_0, V_P and V are the volumes of feed, permeate and retentate, respectively, and C_0, C_P and C, the respective concentrations of the species. I_V and I_C are the imbalances due to absorption or errors for volume and species, respectively. Adapting the process from Wills with only one process unit and one species per minimization, the function to minimize is[14]:

$$S = \sum (I_V)^2 + \sum_i (I_{Ci})^2 \tag{S3}$$

where i stands for each component in solution to be evaluated. However, in this research, only one compound was evaluated at the time. Deriving (S3) for V_P and V, equating them to zero and combining the two derivatives, the following ratio can be obtained:

$$\frac{V_P}{V_0} = \frac{C - C_0}{C - C_P} \tag{S5}$$

which gives new estimated values for V_0, V_P and V using the original mass conservation equations with negligible or zero imbalance.

References

1. S. W. Cowan, R. M. Garavito, J. N. Jansonius, J. A. Jenkins, R. Karlsson, N. Konig, E. F. Pai, R. A. Pauptit, P. J. Rizkallah, J. P. Rosenbusch and et al., *Structure*, 1995, **3**, 1041-1050.
2. H. Nikaido, *Microbiol Mol Biol Rev*, 2003, **67**, 593-656.
3. S. W. Cowan, T. Schirmer, G. Rummel, M. Steiert, R. Ghosh, R. A. Pauptit, J. N. Jansonius and J. P. Rosenbusch, *Nature*, 1992, **358**, 727-733.
4. J. Rosenbusch and R. Müller, *Solubilization of Lipoprotein Complexes. H. Peeters and JP MaSSUC, editors. European Press. Ghent, Belgium*, 1977, 59-68.
5. B. H. Ginsberg, *J Diabetes Sci Technol*, 2009, **3**, 903-913.
6. V. Smuleac, D. A. Butterfield and D. Bhattacharyya, *Langmuir*, 2006, **22**, 10118-10124.
7. J. J. Kasianowicz, M. Kellermayer and D. Deamer, *Structure and Dynamics of Confined Polymers: Proceedings of the NATO Advanced Research Workshop on Biological, Biophysical & Theoretical Aspects of Polymer Structure and Transport Bikal, Hungary 20–25 June 1999*, Springer Netherlands, 2012.
8. H. Ghandehari, P. L. Smith, H. Ellens, P. Y. Yeh and J. Kopecek, *J Pharmacol Exp Ther*, 1997, **280**, 747-753.
9. K. Ling, H. Jiang and Q. Zhang, *Nanoscale Res Lett*, 2013, **8**, 538.
10. L. Lebrun and G. A. Junter, *Enzyme and Microbial Technology*, 1993, **15**, 1057-1062.
11. A. Pluen, P. A. Netti, R. K. Jain and D. A. Berk, *Biophys J*, 1999, **77**, 542-552.
12. O. Baron-Epel, P. K. Gharyal and M. Schindler, *Planta*, 1988, **175**, 389-395.
13. J. J. Choi, S. Wang, Y. S. Tung, B. Morrison, 3rd and E. E. Konofagou, *Ultrasound Med Biol*, 2010, **36**, 58-67.
14. B. A. Wills, T. Napier-Munn and C. Julius Kruttschnitt Mineral Research, 2006, 73-75.